Geofísica Internacional (2018) 57-3: 175-195

Original paper

Application of magnetic method on the Argentine continental shelf between 35ºS and 48ºS

María A. Arecco*, Patricia A. Larocca, Francisco Ruiz, Armando T. Canero and Víctor A. Ramos

Received: July 04, 2017; accepted: March 20, 2018; published on line: July 02, 2018

Resumen

Se analizaron las anomalías del Campo Magnético Total a partir de datos de una red global, con el propósito de contribuir al conocimiento y caracterización de la plataforma continental argentina (35ºS hasta 48ºS). Para ello se utilizaron técnicas de realce, como la señal analítica, el ángulo tilt, y la segunda derivada vertical. Se calcularon las profundidades de las fuentes magnéticas a partir del método de deconvolución de Euler y el modelado de inversión gravimétrica 2D. A partir de los resultados filtrados del TMA se identificaron grandes zonas de fractura de transferencia. La segunda derivada vertical mostró patrones de alta frecuencia en las anomalías G y Tona, así como también en la serie de anomalías M y alineamientos de fondo oceánico, mostrando el carácter volcánico y episódico de los mismos. El método de deconvolución de Euler permitió localizar fuentes magnéticas discontinuas a lo largo del antiguo cinturón Dom Feliciano-Lavalleja, cuyas profundidades van desde 5000 a 8000 m. Se obtuvieron pocas soluciones tipo diques, escalones de falla en las zonas de fallas de transferencia y el borde entre corteza continental y oceánica. Se localizaron fuentes en la serie-M a profundidades entre 8000 y 12000 m. También, este método permitió calcular las profundidades de la conspicua anomalía Tona entre 8000 y 20000 m. Además, a partir de un modelo de inversión gravimétrico 2-D aplicado sobre un perfil con dirección NE, se identificó un cuerpo máfico-ultramáfico a lo largo de la sutura Patagonia-Gondwana hasta casi la superficie. Este cuerpo podría ser una imbricación de la sutura emplazada en rocas del basamento.

Palabras clave: Plataforma Continental Argentina; Anomalía Magnética Tona; Magnetometría; Interpretaciones magnéticas corticales: Terreno Patagonia.

M. A. Arecco*
P. A. Larocca
Instituto de Geodesia y Geofísica Aplicadas
Facultad de Ingeniería
Universidad de Buenos Aires
Av. Las Heras 2214
Buenos Aires, Argentina
*Corresponding author: marecco@fi.uba.ar

F. Ruiz,
Instituto Geofísico Sismológico Volponi
Facultad de Ciencias Exactas Físicas y Naturales
Universidad Nacional de San Juan
Ruta 12 Km 17, Jardín de los Poetas, Rivadavia
San Juan, Argentina

A. T. Canero
Departamento de Física
Facultad de Ingeniería
Universidad de Buenos Aires
Paseo Colón 850
Buenos Aires, Argentina

V. A. Ramos
Instituto de Estudios Andinos
CONICET- Facultad de Ciencias Exactas y Naturales
Universidad de Buenos Aires
Intendente Güiraldes 2160
Buenos Aires, Argentina

María A. Arecco
Escuela de Ciencias del Mar
Instituto Universitario Naval, Armada Argentina
Av. Antártida Argentina 821
Buenos Aires, Argentina

Abstract

The total magnetic anomaly (TMA) from a global grid was analysed in order to characterize the magnetic features of the Argentine continental shelf (35ºS to 48ºS) and to expand the current knowledge of such area. TMA amplitudes within the study area were mathematically filtered and enhanced using various techniques including the analytic signal method, the tilt angle method and the second vertical derivative method. In order to estimate the depths of the magnetic sources on the Tona anomaly and the continental edge, the Euler deconvolution method and a 2-D gravimetric inversion model were applied. The TMA filtering results were used to observe and identify large transform zones such as the Río de la Plata system, the Salado, Ventana, Colorado and Malvinas zones, and other minor systems such as the Rawson transform zones. The San José and El Cortijo crustal sutures were also outlined using the applied methods, and it was possible to map and identify a change in orientation of the Ventania-Cape Fold Belt. The tilt angle method revealed high-frequency patterns in the oceanic crust as a result of its volcanic nature. The second vertical derivative method exhibited high-frequency patterns in the G and Tona anomalies, the M-series magnetic anomalies and oceanic bottom alignments, revealing their volcanic and episodic character through a large and complex distribution of blocks at the continental-oceanic boundary. Discontinuous linear magnetic sources were observed along the ancient Dom Feliciano-Lavalleja shear belt, most of which were calculated by Euler deconvolution to be located at depths of approximately 5000–8000 m. On transform zones, inner alignments and continental-oceanic boundaries, few dipoles associated with fault steps and dykes were identified. The sources of the M-series anomalies were located at depths of 8000–12000 m, whereas abundant deeper sources were identified for the Deseado and Somuncurá massifs and the Mar Argentino rise. The Euler deconvolution method was used to calculate a source depth range for the conspicuous Tona anomaly of 8000–20000 m. In addition, a 2-D gravimetric inversion model based on a NE-trending profile was used to identify a mafic body along the Patagonia-Gondwana suture bounded by a sub-surface. This body may be an imbrication of the suture located in basement rocks.

Key words: Argentine Continental Shelf; Patagonia Terrain; Tona Magnetic Anomaly; Crustal Magnetic Interpretations; Marine Geology.

Introduction

The Argentine continental shelf has a number of distinguishing attributes with a structural history characterized by plate breakup, heat flow and magmatic activity, which have shaped its current tectonic features. The study of magnetic anomalies reveals the structural and lithologic complexity of crustal rocks, providing a window into the geological history of various sectors of the continent, mainly ancient deep-crustal formations whose seismic structures are unclear due to subsequent tectonic and metamorphic activity. The total magnetic anomaly (TMA) of an area allows the main crustal structures, faults, dykes, transform zones and edges or contacts to be rapidly located and characterized (Lefort *et al.,* 1988). Therefore, by utilizing the results of filtering techniques, it is possible to analyse the structure of the Argentine continental shelf, the main offshore basin structures and the continental edge.

Several authors have conducted research in this area, including gravimetric studies of the continental-oceanic boundary (Arecco *et al.,* 2016 *a, b*) and magnetic studies of the continental crust (Ghidella *et al.,* 2005, Max *et al.,* 1999). In addition, investigations such as isostatic compensation and geoid undulation studies in the Claromecó basin (Ruiz and Introcaso, 2011), tectonic studies of the El Cortijo suture zone (Chernicoff *et al.,* 2014; Pángaro *et al*., 2011; Pángaro and Ramos, 2012), seismic studies of margin segmentation (Franke *et al*., 2007) and palaeomagnetic studies (Rapalini, 2005) have been carried out, among other authors.

In this paper, TMA amplitudes were mathematically filtered in the study area and enhanced using various techniques including the analytic signal method (AS), the tilt angle method (TDR) and the second vertical derivative method (SVD), each of which has various advantages in different geologic situations. Applying multiple methods to the same anomaly area improved the reliability of the results. In order to calculate the depths of the magnetic sources in the basement and the crust the Euler deconvolution method was used. In addition, with the aim of creating a tectonic model of the Tona magnetic anomaly sources, 2-D gravimetric modelling was performed based on a transverse profile to the anomaly.

The objective of this study was to carry out a regional magnetic survey of the Argentine continental shelf and its continental margins, including the continental-oceanic boundary (COB) up to the oceanic crust between latitudes of approximately 35ºS and 48ºS. The study area was separated into two smaller zones, the northern (35ºS–41ºS) and the southern (41ºS–48ºS). In this work, one source of total magnetic anomaly was used, a newest global grid EMAG2 satellite grid (Meyer *et al.,* 2016).

Geological setting

The regional structural configuration of the Argentine continental shelf is composed of the Río de la Plata craton located southeast of South America, which extends from the Piedra Alta terrane in Uruguay in the north to the Colorado basin in the south (Pankhurst *et al*., 2003; Cingolani, 2011; Pángaro and Ramos, 2012). This craton is bounded to the east by the Dom Feliciano Belt (Fragoso-Cesar, 1980) and further to the south by the COB (Figure 1 A) (Arecco *et al*., 2016 *a*).

The Archean and Proterozoic-age La Plata Craton by gneisses and meta-igneous complexes is characterized (Ramos, 2008). Accretion occurred along its southern margin involving an amalgamated collage of primarily non-magnetic or weakly magnetic sediments and the metamorphic and igneous micro-continent that forms the Patagonia Platform. Large areas of this crust may have been stabilized during Neoproterozoic to early Palaeozoic times (Tankard *et al*., 1995), but compressional tectonics associated with accretion ceased only during the late Gondwanian orogeny, close to the Upper Palaeozoic (Ramos, 1996).

The Río de la Plata Craton comprises a series of continental blocks that, during the Trans-Amazonian orogeny, were amalgamated (Ramos, 1996). It consists of a series of arc granitoids associated with subduction

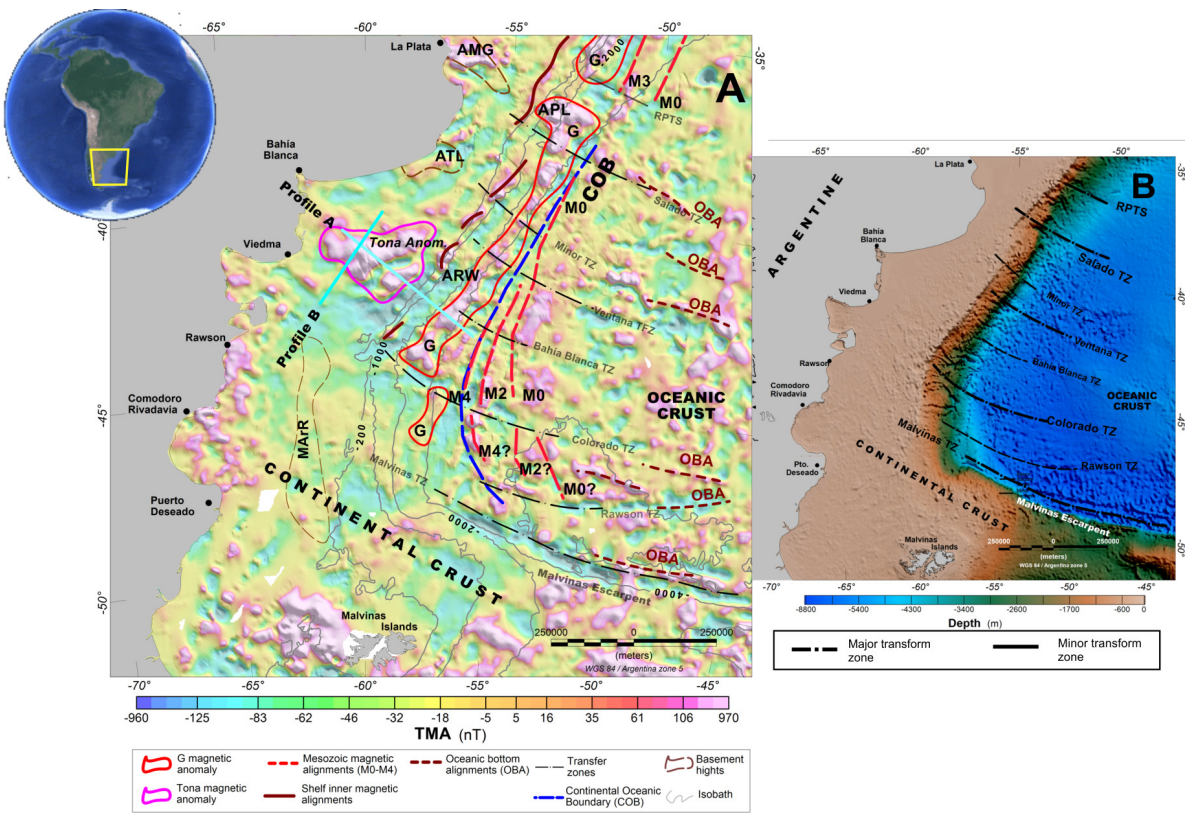

Figure 1. Total-magnetic-field anomaly (TMA) map from the global grid (Meyer *et al*., 2016) (A) and bathymetric global grid map (Amante and Eakins, 2009) (B). In Figure A, the location of profiles through Tona anomaly is marked in cyan lines. TMA map shows the most relevant magnetic anomalies, M0- M4, related to the COB (dashed blue line) and the larger magnetic anomaly, G anomaly (red shut up curve). In Figure B, the main transform zones are depicted. Abbreviations: **COB**: continental–oceanic boundary; **G:** G magnetic anomaly; **M0-M4**: Mesozoic series alignments; **Tona Anom.**: Tona magnetic anomaly; **OBA**: oceanic bottom magnetic alignments; **Salado TZ**: Salado transform zone; **Colorado TZ**: Colorado transform zone; **Rawson TZ**: Rawson transform zone; **Malvinas TZ**: Malvinas transform zone.

preserved in the region of Tandilia (Dalla Salda and Francese, 1985; Dalla Salda, 1987). The granitoid ages range from 2100–1900 Ma in the Tandilia region (Varela *et al*., 1988) (Figure 2). El Cortijo suture runs WNW and is aligned with the northern boundary of the Tandilia terrane (Teruggi *et al.,* 1989, 1988 en el listado de referencias CHECAR;, Cingolani and Dalla Salda, 2000; Cingolani *et al.,* 2010; Chernicoff *et al.,* 2014). At the local scale, El Cortijo suture zone is often E–W-trending. At this scale, WNW-trending tholeiitic dykes (TTD) of Statherian age are seen to cross-cut the Rhyacian El Cortijo suture zone (Chernicoff *et al.,* 2014) (Figure 2). Small magnetic highs that are spatially associated with El Cortijo suture zone are related to unexposed basic ophiolitic bodies related to those present in El Cortijo Formation (Chernicoff *et al.,* 2014).

Several authors have interpreted the presence of a suture related to the collision of the Patagonia terrain (Ramos, 2008; Rapalini, 2005; López de Lucchi *et al.*, 2010, Pángaro and Ramos, 2012) (Figure 2).

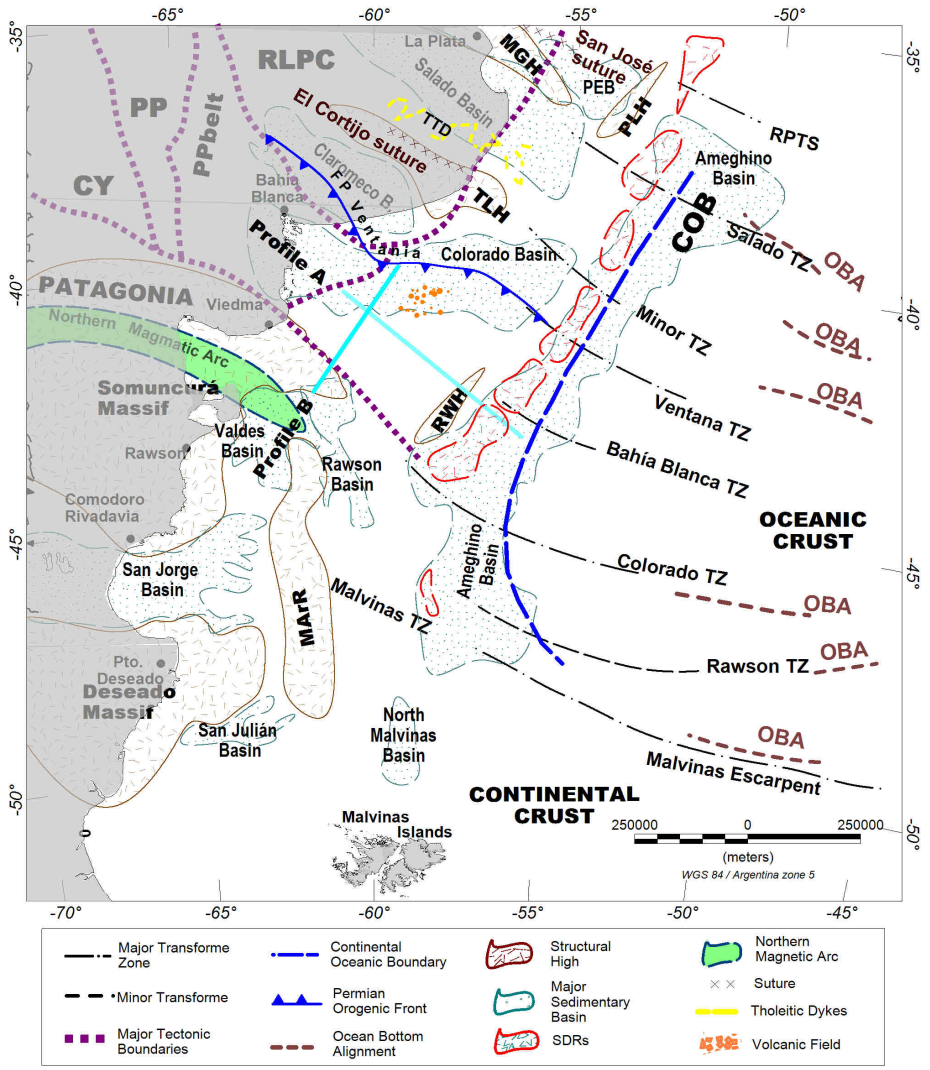

Figure 2. Distribution of the main tectonic structures on the Argentine continental shelf beyond the continental oceanic boundary (COB). The locations of major tectonic boundaries (Pángaro and Ramos, 2012), the Ventania–Cape Fold Belt (Pángaro and Ramos, 2012; Paton *et al.,* 2016), the northern magmatic arc (Ramos, 2008), the COB and oceanic bottom alignments (Arecco *et al*., 2016 *a)*, structural highs and basins (see text for references) are indicated. The main transform zones from Franke *et al*. (2007) and SDR wedges according to Hinz *et al*. (1999) are shown. The Rawson TZ is presented in this work. Abbreviations: **CY**: Cuyania terrain; **PP**: Pampia terrain; **PPbelt**: Pampia belt; **RLPC**: Río de La Plata craton; **Ventania FB**: Ventania Fold Belt; **PEB**: Punta del Este basin; **MGH**: Martín García basement high; **PLH**: del Plata basement high; **TLH**: Tandil basement high; **RWH**: Rawson basement high; **MArR**: Mar Argentino Ridge; **OBA**: ocean bottom alignment.

The passive continental volcanic margin of Argentina began in the Late Jurassic/ Early Cretaceous (~130 Ma) during the last stages of fragmentation of the supercontinent Gondwana, which propagated from south to north. This opening lasted from ca. 137 Ma to 126 Ma (Austin and Uchupi, 1982; Rabinowitz and LaBrecque, 1979) and involved a complex combination of rifting and faulting before and during the breakup of Western Gondwana. This continental margin can be considered a lower-plate passive margin type (LPPM) with the upper-plate passive margin (UPPM) corresponding to the conjugate African margin. The main features characterizing the LPPM-type Argentine continental shelf are expansive shelves, coastal plains in the continental terrace, well-developed half-graben systems, external peripheral ridge systems, and a lack of well-developed basic magmatism, and the presence of extensive rhyolitic plateaux (Ramos, 1996).

The Argentina continental shelf, which begins south of the Colorado River, is one of the best-developed rhyolitic plateaux in the world (Ramos, 1996) with rhyolites corresponding to pre-rift or early-rift types associated with passive margins (Malumián and Ramos, 1984; Kay *et al.,* 1989; Ramos, 1996). The Patagonia microplate is considered to have been independent from Gondwana in the Early to Middle Palaeozoic before it underwent a frontal collision with Gondwana in the Late Palaeozoic, producing folding and thrusting at the Sierra de la Ventana fold system, SW of Buenos Aires (Ramos, 1988, 2008; Rapallini, 2005) (Figure 2).

The G anomaly is considered the biggest among anomalies from Atlantic Ocean opening (Rabinowitz and LaBrecque, 1979); it was drawn in red enclosing positive-negative values because the magnetic field is bipolar (Figure 1 A). Older Mesozoic alignments (M4–M0 off the coast of Argentina) from about 130 to 114 Ma and the G anomaly on conjugate margin offsets (Rabinowitz and LaBrecque, 1979) have been identified from the maximum-minimum zones (warm-cold colors) aligned to the continental margin on updated data (Figure 1 A).

The Tona magnetic anomaly (Ghidella *et al*., 1995) has been identified from its triangular shape between 40ºS and 42ºS (Figure 1A). These is one of several features that have been identified in the Argentine continental shelf, along with the Martín García basement high (MGH) and the Tandil (TLH) and Rawson (RWH) high zones as well as inner alignments oriented sub-parallel to the G anomaly, among others. Regarding the Tona magnetic anomaly, Zambrano (1974) and Urien and Zambrano (1974) stated that "the mesozoic eruptives, so widespread in the Patagonia and western Argentina, are not known to occur in the Colorado basin. They appear on the surface, to wedge out near the southern boundary without reaching the basin itself". Pángaro *et al*. (2011) identified two NE-oriented, NW-dipping deeply rooted shear zones that were mapped all the way to the Moho using wide-angle seismic reflection lines. These shear zones lie to the north of the Tona anomaly. The eastern shear zone is associated with a volcanic field composed of presumably hundreds of volcanoes of Late Cretaceous age, and the south ends of both zones lie just above the northern edge of the Tona anomaly, which could be associated with that volcanic field (Figure 2).

According to Max *et al.* (1999), the northern region (35ºS–42ºS) of the continental crust includes the structural magnetic domain of the Río de la Plata craton (RLPC) and the marginal sub-domain of the La Plata (LPDM) domain that was tectonically reworked during accretion (Somuncurá Massif). These authors affirm that the oceanic crust (OC) contains the M-series and a quiet zone of crust. The RLPC comprises a series of continental blocks that were amalgamated during the Trans-Amazonian orogeny. The sutures run subparallel to San José and El Cortijo and separate the continental blocks of Florida, Buenos Aires and Tandil (Dalla Salda *et al.,* 1988; Teruggi *et al.,* 1988; Ramos *et al.,* 1996).

According to Arecco *et al*. (2016 *a, b*) and Pizarro *et al*. (2016) the continental oceanic transition (COT) and the COB have distinguishing tectonic features, as has been shown in its studies, 2D and 3D gravimetric models, above the Argentine basin and continental boundary (Figure 2). Arecco *et al*. (2016 *a*) showed by 2-D gravimetric models that the continental crustal thinning begins on the continental and transitional crust, where the greatest sedimentary thickness are located, the basaltic wedge series (SDRs), the zone of intrusive magmatic dykes, and the underplated body, till the COB. The 3D model results allowed to obtain the boundaries of the Argentina Basin revealing gravimetric aspects related to the morphology and constitution of the upper crust in the continental margin (Pizarro *et al*. 2016).

In addition, a series of marine basins that resulted from the South Atlantic Ocean opening can be observed in the continental shelf. Among the most important of these are the Punta del Este, the Salado, the Claromecó, the Colorado,

the Valdés, the Rawson San Jorge and the San Julián basins (Figure 2). The half-graben systems on the shelf are strongly controlled by basement features, allowing the shelf to divide into two distinctive sectors by the Patagonic boundary (Figure 2). The northern region of the Río Colorado Salado, Colorado and Claromecó basins was partially developed on the Río de La Plata Craton in the province of Buenos Aires (Dalla Salda *et al.,* 1988; Franke *et al.,* 2007).

The southern region (40°S–48ºS) of the continental crust includes the Somuncurá and Deseado massifs, the northern magmatic arc (Ramos, 2008), slim SDRs and the Valdes, Rawson, Ameghino and San Jorge basins in front of the COB (Figure 2). The Tona magnetic anomaly is large in amplitude but low in frequency; this is in marked contrast to the magnetic pattern over the southern zone, which includes the San Jorge, Valdés and Rawson basins (Figure 1). According to Ghidella *et al*. (1995), "this anomaly was possibly caused by lava flows through detachment faults formed in the rifting process and that these flows seem to have been accumulated against a barrier imposed perhaps by the implications of the Colorado discontinuity". Most of the magnetic oceanic bottom alignments (OBA) are parallel to the TZs, which coincide with the ocean floor spreading direction. Additionally, the magnetic OBAs coincide with the gravimetric OBAs (Arecco *et al*., 2016 *a*).

Several authors such as Zambrano (1974), Introcaso and Ramos (1984), Tavella and Wright (1996), Fryklund *et al*. (1996) and Introcaso *et al*. (2008) have discussed the geology of these basins, originated during a major rifting event in the Late Jurassic and Early Cretaceous, among others. In the southern region of the Río de la Plata craton is the Gondwanides mountain belt, which was produced as a result of the late Palaeozoic collision of the Patagonia terrane with the continental margin of Gondwana (Ramos *et al.,* 2014) (Figure 2). The southern part of the Colorado River marks the edge of an important area of acid volcanism, but also an area structurally dominated by meridian-parallel half-grabens, as observed in the Valdés and Rawson basins (Marinelli and Franzin, 1996). In the south, transverse structures are found corresponding to the marine section of the San Jorge basin (Baldi and Nevistic, 1996, Sylwan, 2001). The Somuncurá massif adjacent to the shelf contains a series of outcrops of lava and pyroclastic flows of rhyolitic composition associated with granitic porphyry. Recent dating work performed by Riley *et al*. (2016) in rocks from the Marifil Formation yielded similar ages. The northern sector of the Somuncura massif is considered to be a magmatic arc that was active along the northern edge of the plate prior to collision between the Patagonia block with Gondwana (Ramos, 2004, 2008). OBAs in the oceanic crust have been identified from TMA anomalies, as well as from gravimetric anomalies and through the application of enhancement techniques (Arecco *et al.,* 2016 *a, b*).

Methodology

The main TMA magnetic data source is the EMAG2 satellite grid, which is available as a digital file at https://data.noaa.gov/dataset/emag2-earth-magnetic-anomaly-grid-2-arc-minute-resolution (Figure 1 A). These data are available with a grid spacing of 2 arc-min (~ 4 km in the study area). This grid has been compiled from satellite data, ship and airborne magnetic measurements according to Meyer *et al.* (2016).

Enhancement techniques used include the analytic signal (AS), the tilt angle (TDR) and the second vertical derivative (SVD) methods, as well as 3-D Euler deconvolution to obtain the location and depth of the faults or dykes (edges or contacts) of the main tectonic structures. Finally, a 2-D Euler deconvolution, and 2-D gravimetric model were applied on a transverse profile to Tona anomaly for obtaining causative source depth.

Analytic Signal

The 2D technique developed by Nabighian (1972) was applied to magnetic potential fields. The author later generalized the analytic signal (AS) from 2D to 3D (Nabighian, 1984). This technique indicates the relative maxima at the contact between bodies with different magnetic susceptibilities. In particular, the analytic signal module $|\mathrm{AS}|$, also termed the total gradient (Nabighian *et al.,* 2005), has been used to detect maxima at the contact between bodies with different magnetic susceptibilities. The amplitude of the $|\mathrm{AS}|$ module in 3D is given by (1)

$$|AS| = \sqrt{\left(\frac{dTMA}{dx}\right)^2 + \left(\frac{dTMA}{dy}\right)^2 + \left(\frac{dTMA}{dz}\right)^2} \quad (1)$$

where $\frac{dTMA}{dx}, \frac{dTMA}{dy}$ are the horizontal derivatives and $\frac{dTMA}{dz}$ is the vertical derivative

of the TMA. Each |AS| maximum indicates a contact between bodies of high magnetic susceptibility contrast.

Tilt angle (TDR)

The enhancement technique introduced by Miller and Singh (1994) to detect contacts when applied to the Total Magnetic Field grid (Verduzco *et al.,* 2004) provides greater resolution of the edges with respect to those shown by the AS. This filter is able to detect depth sources masked by high-amplitude interference from superficial magnetized bodies. The tilt angle (TDR) is given by expression (2)

$$TDR = \tan^{-1} \frac{VDR}{THDR} \qquad (2)$$

where VDR and THDR are the first horizontal and the vertical derivative of the TMA, respectively (Verduzco *et al.,* 2004). A TDR value of zero indicates an edge or contact. Due to the nature of the tangent function, all resulting angles are in the range between $-\pi/2$ and $\pi/2$ (Cooper and Cowan 2006), so that the details of other contacts whose angles are not close to zero are lost.

Second vertical derivative

The second vertical derivative (SVD) is the vertical gradient of the first vertical derivative, which is physically equivalent to measuring the magnetic field simultaneously at two vertical points, one above the other, by subtracting the respective values and dividing the result by the vertical spatial separation between the measuring points (Blakely, 1996). In the wavenumber domain, the 2nd-order vertical derivative is given by (3)

$$A' = A(k)|k|^2 \qquad (3)$$

where *A(k)* is the amplitude at a wavenumber *k* ($k = 2\pi/\lambda$) and λ is the wavelength (Blakely, 1996). The result enhances relatively high frequencies in contrast to low frequencies. The vertical derivative exaggerates the signal of the upper-level sources producing magnetic anomalies. This property is the basis for applying the derivative, which eliminates the regional effects of long wavelengths and enhances the effects of shallow surface bodies. Implementation of the second vertical derivative requires good quality data as the enhancement of high frequencies may result in increased noise (Milligan and Gunn, 1997).

Euler deconvolution method

The Euler deconvolution method provides the location and depth of the magnetic source tops. The Euler deconvolution method for estimating the depths of magnetic sources is based on the concept that magnetic fields are homogeneous functions of the source coordinates and therefore satisfy the Euler equation. This equation can therefore be solved parametrically to determine the source locations. This method has found widespread application as the theoretical basis for the inversion of large magnetic and gravity data sets in terms of simple sources in the shape of steps, spheres or cylinders (Thompson, 1982; Reid *et al.,* 1990; 2003; Salem and Smith, 2005). When the structural index and estimated depth are combined with geologic information, they can be used to identify and estimate the depths of a wide variety of geologic structures such as faults, magnetic contacts, dykes and extrusions, among others (Thompson, 1982).

The Euler deconvolution method is based on the Euler homogeneity equation, which can be written in 2D in the form

$$\left(x - x_0\right)\frac{\partial TMA}{\partial x} + \left(z - z_0\right)\frac{\partial TMA}{\partial z} + \eta TMA = 0 \qquad (4)$$

where the total magnetic field anomaly (*TMA*) is due to a magnetic source located at (x_0, z_0) and η is a structural index (SI) (Table 1) related to the simple source geometry. The only unknown quantities in equation (4) are x_0, z_0 and η. The depth and location along the profile are represented by the coordinates while η represents the type of source.

To solve Euler's equation, horizontal and vertical potential field gradients are required, which were calculated in the frequency domain (Gunn, 1975). It has been observed that depth estimates that are obtained from magnetic data are more accurate if the reduced to pole (RTP) magnetic field is used (Thomson, 1982).

Table 1. Structural indices in 2D and more common symbols used to represent the indices.

Structural index	Simple model	Symbol
1.0	Fault or contact	+
2.0	dike	×
2.5	dipoles	□
3.0	sphere	^

2-D model inversion

In spite of ambiguity that the inversion of the gravimetry presents, for the construction of a tectonic model, the realization of tectonic models based on the inversion of gravimetric models is efficient. To overcome the non-uniqueness problem, it is possible to invert gravimetric data with a priori information about the crustal structure to provide additional constraints, such as discontinuities from seismic refraction studies or seismic horizons interpreted from multichannel seismic profiles (Nabighian *et al*., 2005). In the inversion performed for the 2-D gravimetric model in this study, a structure based on simple crustal blocks was assumed, from previous works (Pángaro and Ramos, 2012; Ramos *et al*., 2014). For this purpose the Grav-Modeler program, based on Talwani *et al*. (1959) and developed by the Geotools software division of AOA Geophysics Inc. and Lacoste & Romberg, was used.

Results

The differences in magnetic susceptibility of structures such as faults or steps, dykes or sills generate different magnetic responses. For the purpose of differentiate geological structures in the crystalline basement and upper crust enhancement techniques of magnetic anomalies were used. In order to display the results more clearly, the study area was divided into two zones (35ºS–42ºS and 40°S–48ºS) as shown in Figures 3, 4 and 5. The results of the 3-D Euler deconvolution can be seen in Figure 6. Additionally, in order to identify the sources responsible for the Tona anomaly, two cross-sectional profiles, A and B, were made. Profile A was oriented in the NW–SE direction and was processed by an Euler deconvolution performed in 2D (Figure 7). Profile B was made in the NE–SW direction, and was used to create a 2-D gravimetric model (Figure 8).

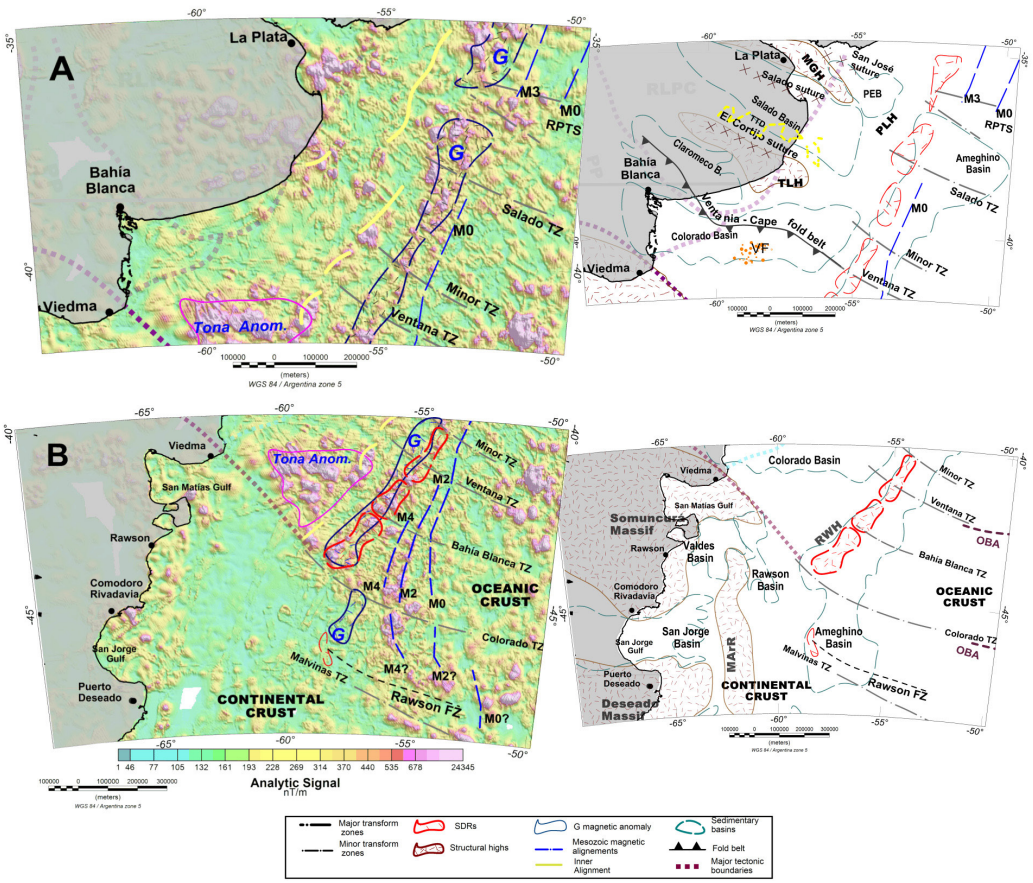

Figure 3. Analytic signal maps of the northern zone (A) and the southern zone (B). The respective geologic maps are located to the right of the AS maps. The Rawson transfer zone is enhanced and presented in the analytic signal map. Magnetic alignments were identified using enhancement techniques. For references of geological structures, see the title Geological setting. Abbreviations: **RPTS:** Río de la Plata Transform System; **VF:** volcanic field; **PLH:** del Plata high; **MArR:** Mar Argentino Ridge; **TTD:** tholeiitic dykes; **OBA:** ocean bottom alignments. For others references see Figures 1 and 2.

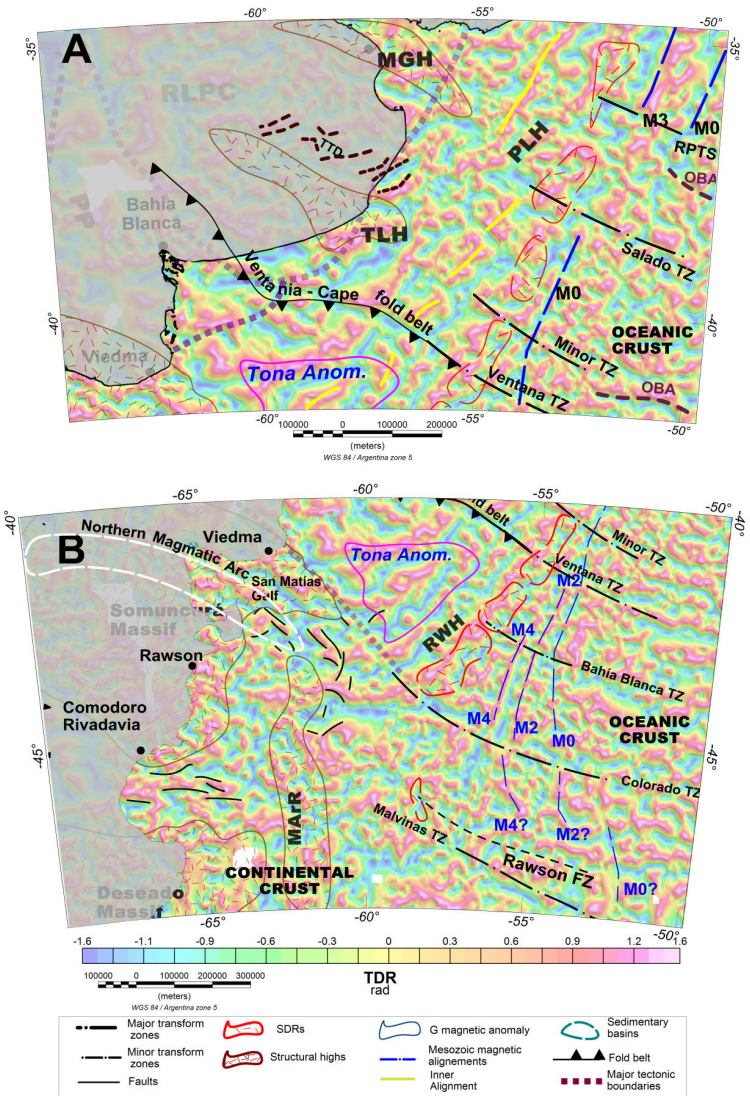

Figure 4. Tilt angle (TDR) maps of the northern zone (A) and the southern zone (B). In the northern zone, various boundaries are enhanced by TDR because the null values indicated edges, as the southern edge of the Colorado basin, the Tandil High, the THD and inner alignments. In the southern zone, the tilt angle enhances the Minor Transform transform zones and some faults in the Valdés, Rawson and San Jorge basins. Abbreviation: **TTD:** tholeiitic dykes. For others references see Figures 1 and 2.

Analytic signal

The analytic signal shows the magnetic contact responses by high values (magenta) (Figures 3 A; B). Structures associated with crystalline basement such as the Martín García and Rawson basement highs can been seen, while the Tandil basement high appears less distinct. In addition, the AS depicts an eastward shift of the G anomaly in the Río de La Plata Transform System zone understanding of a control of system about G anomaly (Figure 3A). The Tona anomaly appears as a triangular magnetic high with its somewhat subparallel edge to the magnetic G anomaly to the east, Patagonia boundary to the south and Colorado Basin to the north. Note that, the Tona anomaly exhibits long wavelengths that prevail over short wavelengths, i.e. its sources probably are deep. In Figure 3B, alternating alignments with very high values (magenta) and low values (green) can be identified subparallel to the continental margin representing the Mesozoic seafloor spreading alignments M0–M4 (Rabinovich and LaBrecque, 1979). A detailed analysis of the analytic signal map (AS) corresponding to the northern region shows NE–SW alignments with high values between 1000 and 500 nT/m corresponding to the continental edge (Figure 3A).

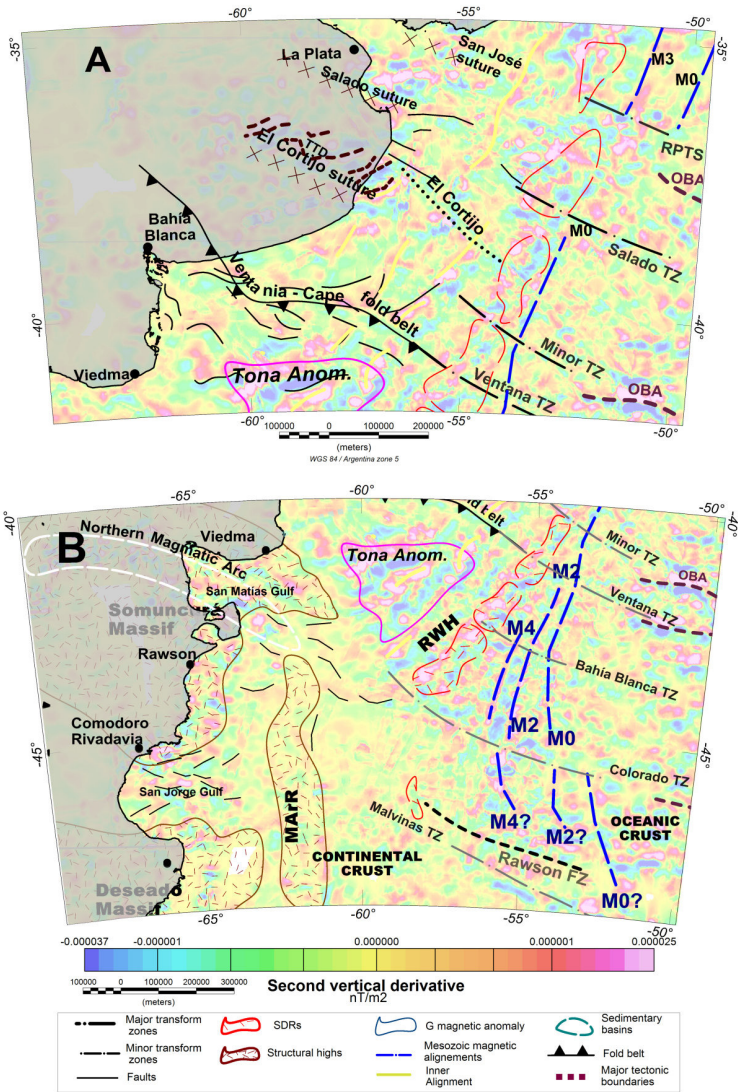

Figure 5. Second vertical derivative (SVD) map of the northern zone (A) and the southern zone (B). In the northern zone, a pattern of high frequency is seen in the continental crust, such as in the basement high of the Martin García and Tandil basins, and in the areas of the G and Tona anomalies and the TTD. SVD exhibits a rough and broken pattern in areas of the oceanic crust such as the Mesozoic alignments and the OBA. Abbreviation: **TTD:** tholeiitic dykes. For others references see Figures 1 and 2.

The Salado basin is described as aulacogenic rift basin, and exhibits a NW–SE-oriented fault pattern (Ramos, 1996; Urien and Zambrano, 1974) (Figure 3 A). The southern edge displays different values ranging from 200 to 800 nT/m, while the northern edge borders the Martín García Precambrian outcrop threshold (Ramos, 1996; Urien and Zambrano, 1974) reaching values up to 1000 nT/m. The eastern edge is represented by a series of faults in the Plata High (Ramos, 1996) with values of up to 1200 nT/m. The AS shows that the Martín García basement high controls the features of the Salado and Punta del Este basins (Ramos, 1996). The north slope of the Punta del Este basin is controlled by WNW-ESE alignements orientated parallel to the San José suture (Ramos, 1996), which is bounded to the east by the G magnetic anomaly and to the north by the Martín García basement high.

North of El Cortijo suture in the continental zone, the AS reveals a sheet-complex with a NW–SE orientation controlled by the Salado transform zone. This area of WNW-trending tholeiitic dykes (TTD) (Chernicoff *et al*., 2014) extends towards the shelf and beyond the coast and changes to a predominantly N–S orientation due to a rotation associated with the onset of the

Figure 6. 3-D Euler deconvolution fault maps of the northern zone (A) and the southern zone (B). Depths of the faults are represented by green circles. The circle's size is related to the depth of the source. Abbreviation: **SI:** structural index. For others references see Figures 1 and 2.

South Atlantic opening (yellow lines) (Figure 3 A). In contrast, parallel to the Salado transform zone (Salado TZ) and the Río de la Plata system (RPTS), the AS displays thin transform zones that influence most of the G anomaly, as can be seen in the Minor TZ and the Patagonia-Gondwana suture.

On the southern edge of the Colorado Basin, the AS displays higher values in the range of 1200–2000 nT/m (warm colors), which reveal the deepest volcanic sources coinciding with the Tona magnetic anomaly to the northeastern of the Somuncurá massif. The Tona anomaly borders a volcanic basement high comprised of deep volcanic rocks, so the amplitude of the SA indicates a deep souce of the volcanic field toward the ocean bottom.. The offshore Somuncurá Massif on the continental shelf (Ramos, 1996) has similar characteristics to the onland Somuncurá Massif, which is part of Patagonia (Río Negro and central Chubut). Therefore, the Tona anomaly represents the boundary of the offshore massif on the continental shelf. This massif contains a series of outcrops of lava and pyroclastic rhyolitic flows associated with granitic porphyries. Given its lateral extent of several hundred kilometers in diameter, the formation of this massif could be related to asthenospheric hot-spot activity that partially melted the upper crust during an extensive period of pre-rift magmatism associated with the initial opening of Southern Atlantic (Rapella and Pankhurst, 1993).

The Rawson structural high (RWH), which controls the southeastern edge of the Colorado Basin, reaches values of 2000 nT/m. The western edge of the Colorado basin is parallel to the continental edge, with structural highs reaching values from 800 to 1000 nT/m. The northern edge of this basin exhibits values of 100 to 200 nT/m (cold colours), whereas the submerged area in front of the coast between Bahia Blanca and Viedma exhibits the lowest values in the study area, around 50 nT/m. Low anomalies are seen along the northern edge because this area is in contact with the Palaeozoic Claromecó basin, which is a sediment-sediment transition rather than the sediment-intrusive transition seen in the south and the east (Ruiz and Introcaso, 2011).

The more prominent features in the southern region (Figure 3B) include the Somuncurá and Deseado massifs, Mesozoic magnetic anomalies and the Malvinas transform zone. These features display values from 1500 to 2000 nT/m. In this region the G magnetic alignment is sub-parallel to the continental edge and is interrupted at 44ºS and at 45ºS by the Colorado TZ and the Rawson TZ, respectively. An arc-shaped high-frequency pattern with a primaryily E–W orientation (~41ºS) can be identified from the continent to the Golfo San Matías, which is then interrupted by the Colorado TZ (Figure 3B).

The N and S edges of the San Jorge basin exhibit the highest values in the basin, reaching approximately 400 nT/m. No information for the eastern edge of the basin is available. The AS indicates that the features at the edges of these basins are controlled to the north by the Somuncurá massif, to the east by the Colorado TZ and in between by the Mar Argentino Ridge (MArR) (Rolleri, 1972). The AS does not show the extensive faulting typical of basins formed in the mid-to-late Jurasic during rifting between South America and Africa. A fan pattern can be observed in the magnetic alignments, along with a shift to the east due to the opening of the South Atlantic Ocean. The Rawson transform zone extends eastward parallel to the Colorado Transform zone in the south. This transform zone controls the Mesozoic alignments (M4 and M2) north of the Malvinas Transform zone.

Tilt angle

The tilt map resulted in improved determination of edges, contacts or faults identified in the AS, such as the basin axis extension, the shape and extension of sutures, the El Cortijo TZ and minor and the RPTS (Figure 4A). The tilt angle can discriminate between oceanic and continental crust by the high-frequency pattern in oceanic crust. The tilt angle map of the northern zone delineates various sources and provides information about the northern and southern edges of the Punta del Este basin. In addition, the southern and eastern edges of the Colorado basin are clearly marked, as well as the southern edge of the Claromecó basin. Moreover, the basin axes of the Punta del Este, Salado and Claromecó basins can be clearly observed. In the oceanic crust, TDR enables identification of the M3 alignment, although TDR does not allow OBAs to be clearly identified (Arecco *et al.,* 2016 *a*). However, the TDR application did enhance the outline and extension of El Cortijo suture from the continental shelf to the edge through its influence on the G anomaly. Furthermore, high frequencies on the inner side allowed identification of fractured blocks as a result of the amalgamation of the continental blocks that comprise the suture surrounded by the extended El Cortijo suture to the NW. El Cortijo suture is highlighted in the WNW–ESE direction in the TDR map, along with TTD of Statherian age. The Patagonia-Gondwana suture is clearly demarcated up to the G anomaly and the tilt angle map shows oblique alignments in the general direction of the Patagonia terrain tectonic edge. Between the G anomaly and the shoreline, inner alignments sub-parallel to the margin can be seen that are controlled by the Salado, Ventana and minor transform. These inner alignments were probably activated by the opening of the South Atlantic Ocean.

In the southern area, null values are observed along the eastern and southern edges of the San Jorge Basin, and the northern and southern edges of the Rawson and Valdés basins are clearly marked (Figure 4B). Using this enhancement technique, the magnetic G anomaly and the NE–SW-orientated parallel magnetic alignments M4, M2 and M0 can be recognised as high-frequency alignments. South of the Colorado TZ, an eastward shift in these main alignments can be observed where the G prolongation is clearly identifiable by the change to a N–S orientation. Similarly, a change in the orientation of the Mesozoic M4, M2 and M0 alignments can be observed parallel to G (Figure 4B). Above this continental crust, the Rawson TZ is seen to limit the southward continuation of the G anomaly as well as that of the Mesozoic magnetic alignements running parallel to the Colorado TZ and the Malvinas TZ (Figure 4B). Therefore it can be concluded that the Rawson TZ was activated during the opening of the Atlantic Ocean. Above the oceanic crust, oceanic bottom alignements (OBA) can be identified, thus confirming the expansion direction in the oceanic bottom region (together with the orientation of transform zones).

Second vertical derivative

The main features highlighted in the results of the SVD implementation are associations between weak zones, like cortical faults (San José and El Cortijo sutures), or the magmatic arc in the Nordpatagonic massif (Figures 5A and 5B). Magnetic fabric edges are highlighted by a high-frequency pattern, as in the G and Tona anomalies. Additionally, it was possible to distinguish two types of organization in the patterns of the SVD frequencies between the continental and the oceanic crust. In the oceanic crust, a magnetic fabric with high-frequency patterns was observed with particularly clear alignments subparallel to the edges such as in the G, M0, M2 and M4 alignments. These are crossed by transform zones perpendicular to the crustal boundary, some of which are associated with transform zones (Salado and Colorado TZ). A heterogeneous fabric was observed in the continental crust, where low-frequency patterns are associated with large structures.

In the Tona anomaly, the magnetic fabrics appear as a series of maxima and minima alignments with NE–SW orientations. Intrusive dykes of magmatic material can be better seen in the NW–SE profile across the Tona anomaly (Figure 7). To the north of the Salado basin, the SVD depicts the edges of the Martín Garcia Precambrian basement by a high-frequency pattern (Figure 5A). As seen in the analytic signal (AS), the high-frequency pattern in the G anomaly is interrupted by the RPTS, while in the SVD map, a group of contacts displaced to the east were observed that were likely activated during the Atlantic Ocean opening (Figure 6A).

The SVD map allows TTD contacts of the Statherian age to be clearly identified due to a greater contrast between alignments running transverse to El Cortijo suture, which are bounded to the North by the Salado basin and to the South by the Tandil Highs (TLH) (Figure 5A). In the southern area (Figure 5B), the SVD highlights the G anomaly, M0–M4 and the Somuncurá massif contacts as a pattern of high frequencies. These fan-shaped Mesozoic series alignments appear to be bounded to the south by the Colorado TZ, while in the southern Colorado TZ the G anomaly and Mesozoic alignments M0–M4 appear as a disorganized high-frequency pattern strongly controlled in between by the Colorado TZ and tge Rawson TZ, which is not visible in the AS and TDR maps. In the southern area (Figure 5B), SVD allows the contact between the western edge of the Rawson basin and the Precambrian basement of the Mar Argentino ridge (MArR) to be seen, as well as contacts underlying failed rift structures.

Although all the techniques of highlight identified the edges or contact magnetic sources, the Second Vertical Derivative, highlighted them with higher resolution.

3-D Euler deconvolution results

A 3-D Euler standard deconvolution was applied to the magnetic field anomalies in order to provide information about the location and depth of faults and dykes or sills. For the study area, the Euler deconvolution was calculated with two structural indices (SI), SI=0 and SI=1, which correspond to faults and dykes or sills respectively. It was calculated with window sizes of 5000, 12000 and 20000 m, and all depth solutions with error estimate smaller than 15 % tolerance were accepted using the algorithm of Extended Euler provided by GETECH based on Mushayandebvu *et al*. (2001).

Euler's solutions are represented as circles, faults (green circles) and dykes (orange circles); the circle's diameter is related to the depth of the source, the greater the diameter, the bigger the depth (Figure 6).

The deepest faults, between 14,000 and 18,000 m depth, appear where the opening tectonic movement left the most evident features such as, to the north, in the M0 and M3 mesozoic magnetic alignment zones, and in the transform zone of the Salado and in the Río de la Plata transform system (RPTS) (Figure 6). Others, as deep as the previous ones, occurred within the basins of Salado, Colorado, Rawson, Valdés and San Jorge, confirming their stretching patterns (Figure 6). Along the Rawson Basin, the Ventania-Cape fold belt and the Tona anomaly, there are faults or steps, perhaps denoting the accretion of the Patagonia to Gondwana terrain around 8000 m deep. Steps less than 6000 m deep are visible in the Martín García, del Plata and Tandil basament highs, while in the Rawson high they reached more than 14000 m (Figure 6). Traces of tectonic activity are denoted in San Jose and El Cortijo sutures, and other faults or steps less than 2000 m in the Punta del Este basin (PEB), and scattered solutions indicate the eastern edges of these basins at approximately 1500–2500 m (Figure 6).

The dykes reveal volcanic activity, so it is consistent to find solutions in areas such as sea floor expansion or transform zones. In this work dike's solutions or sills were found very deep to more than 14000 m deep, that probably are associated to the zones of opening of the South Atlantic Ocean, like the alignments of the Mesozoic M0-M4, and to the basaltic wedges SDR. Also, there are numerous dykes

at 10000 -12000 m, in the Northern Magmatic Arc, Somuncurá massif, the zone of the Tona anomaly and basament high, this last separates the Valdés and Rawson basins.

Most dyke solutions are very deep at around 10000–16000 m below sea level. Few solutions reach 3500 m. Dyke solutions located in the continental crust such as the G anomaly next to the Republic of Uruguay, the areas south of the Tandil high and in the Colorado, Claromecó and Salado basins and the Tona anomaly reach 14000 m (Figure 7A). Estimated source depths in the Somuncura massif, the Northern Magmatic Arc (Ramos, 2008) and the MArR reach ~16000 m (Figure 7).

Numerous solutions are present at 40ºS–48ºS near the Mesozoic magnetic alignments (M0, M2 and M4) between depths of 11000 and 8500 m, corresponding to the magnetic fabric of seafloor spreading. These solutions agree with the high-frequency patterns in the SVD map. They seem to be controlled by minor, Ventana, Rawson, Colorado and Malvinas transform zones (Figure 7A).

Inside the San Jorge, Rawson and Valdes basins, some faults were detected at various depths from 500 to 2000 m. Deeper sources can be observed in the Deseado massif at 3500 m depth (Figure 7B).

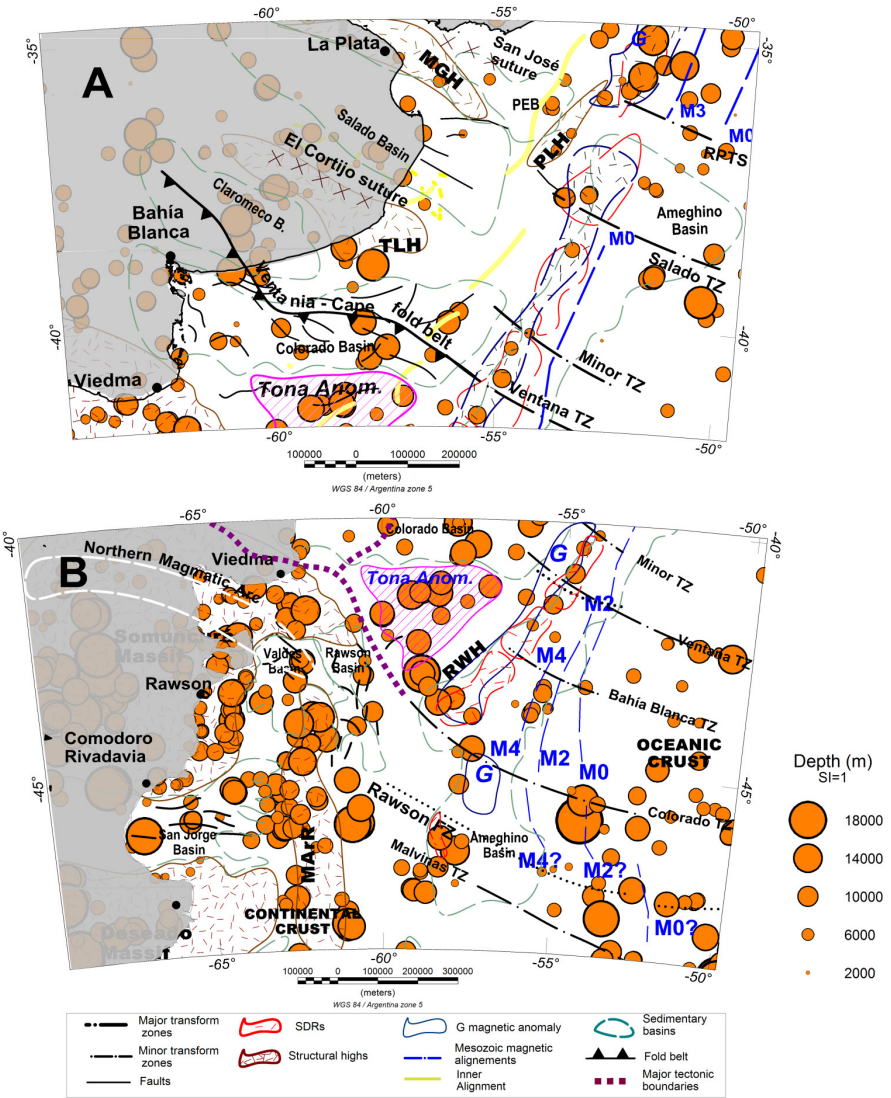

Figure 7. 3-D Euler deconvolution dyke maps of the northern zone (A) and the southern zone (B). Depths of the dykes are represented by orange circles. The circle size is related to the depth of the source. Abbreviation: **SI:** structural index. For others references see Figures 1 and 2.

However, it should be noticed that the Euler source faults are the result of a simple mathematical model and do not necessarily indicate the presence of real geological faults or contacts, for example, in the sea sources deeper than 12000 m. Consequently, it should be taken into account that all Euler calculations only depict real distributions of magnetic material in those cases supported by geological and geophysical models such as basement highs, volcanism or basaltic flows.

2-D Euler deconvolution of Tona anomaly

In order to perform a detailed analysis of the structures comprising the Tona anomaly and the G anomaly up to the COT (profile A, see location in Figure 1A) a 2-D Euler deconvolution was applied. To find the solutions corresponding to faults or steps and dykes or sills, the equation of Euler's deconvolution in 2D was solved using the software presented by Durrehim and Cooper (1998). The structural indices used were, SI= 1 and SI= 2 with windows of 7000, 9000 and 15000 m; the faults and the dykes were identified by the (+) and (×) symbols respectively.

The TMA (black line) and the reduction to pole (RTP) profiles (red dashed line) are shown in the top of Figure 8 from which the zones of the Tona magnetic anomaly and the G magnetic anomaly (green arrows) were identified. The lower part of the figure shows the calculated solutions for faults (+) and dykes (×). In addition, the locations encased in green ellipses, solutions associated with the subplated bodies were marked and within the yellow ellipses, the dykes related to the base of the SDRs were identified in the COT zone. Besides, the solutions, such as contacts with the SDRs (1000 - 5000 m) or basement highs (2000 - 5000 m) coincided with seismic studies (Hinz *et al*., 1999).

The Euler solutions interpreted were calculated considering a window width of 7000 m, as shown in the lower part of Figure 8. Most of the shallow solutions under the Tona magnetic anomaly, are located at 1000 m depth, in coincidence with the crystalline basement according to Ewing *et al*. (1963). However, considering the amplitude and wavelength of the reduction to the pole, the most probable solutions are the deepest ones, greater than 10000 m depth.

Moreover, the observed solutions between 1000 and 10000 m depth are associated with dykes and intra crustal chimneys of volcanic material caused by lava flows that filtered up towards the seafloor due to greater tectonic activity.

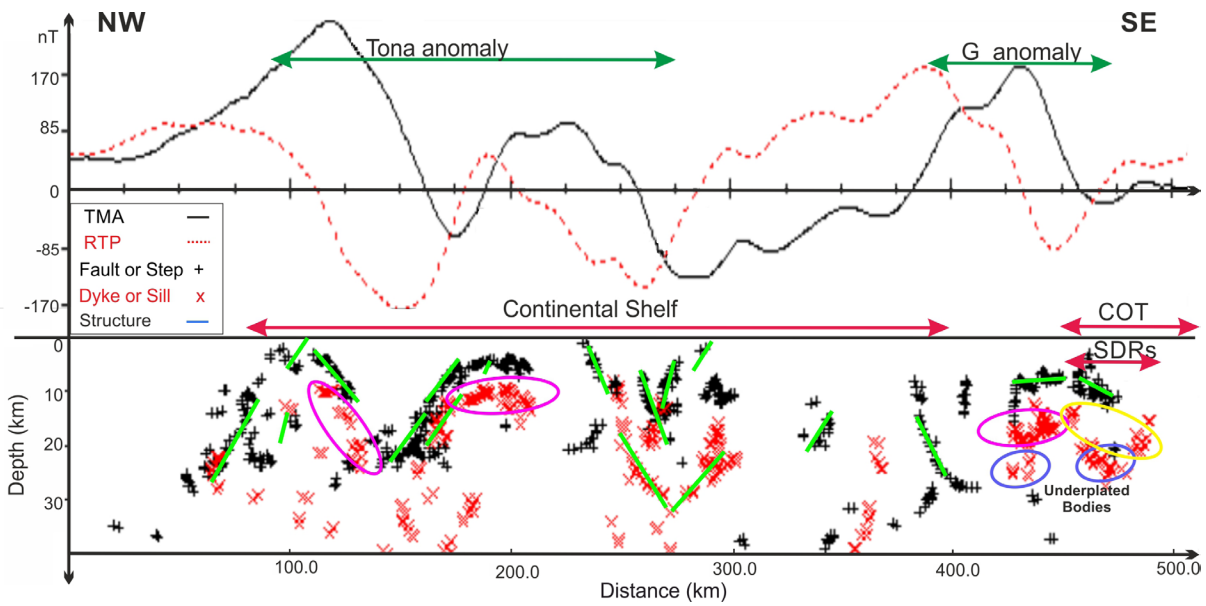

Figure 8. Profile A through the Tona anomaly and the G anomaly. Upper part: TMA and RTP are shown. Lower part: Euler deconvolution solutions are interpreted. The interpreted green lines show the solutions of likely faults and dykes. Ellipses show particular structures, such as underbodies (in blue), feeding dykes zone (in yellow) or dykes/sills under Tona and G anomalies (in magenta). Abbreviations: **COT:** continental oceanic transition; **SDRs:** seaward-dipping reflector series (see location of profile A in Figure 1A).

2-D gravimetric inversion model of Tona anomaly

The 2-D gravimetric model, applied to the Tona anomaly's area of influence (profile B, see location in Figure 1A), was a technique that contributed to the explanation of the causative sources of the conspicuous Tona anomaly. Together with the magnetic field analyses it was used to deduce the tectonic conformation of the Patagonia Suture (Figures 9 A; B). To overcome the non-uniqueness problem, a 2-D gravimetric inversion model can be applied with a priori crustal structure information as a constraint. This 2-D gravimetric inversion model is taken from a structural cross section of the Gondwanides of northern Patagonia, taken from a small portion of a study of the Palaeozoic Ventania System (Ramos *et al*., 2014). The interland region developed in the present-day Somuncurá massif with exhumed late Palaeozoic arc-granitoids is shown, as well as the Ventania System with its fold and thrust belt and the associated Colorado basin. The lower part of Figure 9B shows the magnetic profile (black line), the observed gravimetric profile (green circles) and the calculated profile (blue line). The lower part of Figure 9 shows the 2-D gravimetric inversion model. This model represents a new interpretation of the blocks that may generate the Tona anomaly.

From left to right in the 2-D model are the continental block of Patagonia and the ancient suture with the Gondwana continent (Patagonia-Gondwana suture). Downwards, the 2-D model displays alternating large sedimentary layers termed Palaeozoic sediments (possible

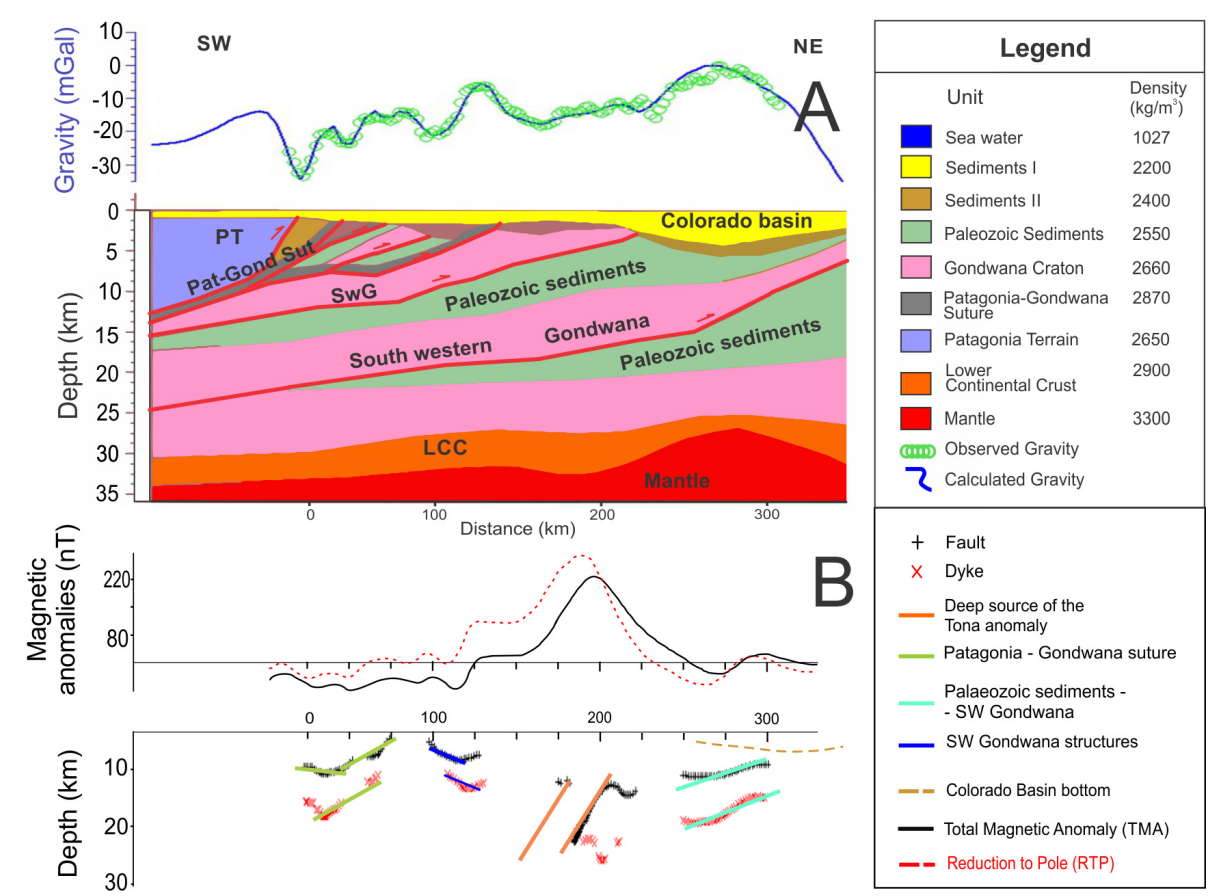

Figure 9. Profile B through the Tona anomaly. 2-D gravimetric model (A) and magnetic deconvolution (B). In Figure A, the observed free air anomaly (green circles) and calculated gravity (blue line) were depicted on top. The gravimetric model's rms is ±2.5 mGal. The density values used in the 2-D gravimetric model are listed in the legend. Red lines highlight the contours of the failed Patagonian suture (see profile B location in Figure 1A). In Figure B, Euler deconvolution solutions, contacts/faults by (+) and dykes/sills by (x) are represented. The interpreted lines are according to failures Patagonia-Gondwana Suture and others failures. Abbreviations: **PT:** Patagonia Terrain; **Pat-Gond Sut:** Patagonia-Gondwana suture; **SwG:** South western Gondwana; **LCC:** Lower continental crust.

accretionary wedges) and detachment faults generated during the accretion phase. The 2-D gravimetric inversion model indicates the presence of a sub-horizontal dyke of volcanic material from the Patagonia-Gondwana suture running parallel to detachment faults that formed during the Patagonia accretion process

The deconvolution of Euler 2-D, applied to the throught profile (profile B) to the magnetic anomaly Tona contributed to obtain the depth of the causative structures (faults and dykes) under the area of influence of the conspicuous Tona anomaly. This method, joint with the 2-D gravimetric inversion, allowed finding a sustainable model of the deep structures of the Tona anomaly.

The gravimetric profile shows a high on the Colorado basin, which is produced by the rise of Mohorovičić discontinuity. The density contrast between the continental crust and the mantle is enough to provoke it. This phenomenon has been studied by Introcaso (1980, 2003) in the Salado and Colorado aulacogenic basins.

Conclusions

The magnetic method presented here, based on a combination of enhancement techniques and 3-D Euler deconvolution, have been used for rapid identification of the main structures on the Argentine continental shelf between 35ºS–48ºS. In addition, 2D studies were used to determine the depths of the blocks that generate the Tona anomaly.

The older Mesozoic alignment series (M4–M0) off Argentina (from ~130 to 114 Ma) and the G anomaly were identified and re-mapped according to modern data. By using techniques applied to TMA in oceanic crust, OBA, major transform zones, minor transform zones and new transform zone such as the Rawson was able to be accurately identified. The use of different techniques, including 3-D Euler standard deconvolution, allowed to highlight various aspects of each of these structures, such as the shallowness, depth, size, trend and extension. 3-D Euler deconvolution provided the depths of the causative sources of the features such as TTD, crystalline basement highs, the Tona anomaly, inner alignments main faults and some basin edges were accurately identified on the Argentine continental crust.

Both the AS and TDR clearly displayed contacts between the highest magnetic susceptibility contrasts such as the G anomaly, which is controlled by the RPTS, Salado, and Colorado transform zones as a result of Gondwana break-up. By applying AS, TDR and SVD it was possible to view the individual M-series features more distinctly between the Colorado and Rawson transform zones in the area from 35ºS to 42ºS. This separation results from extension during the break-up of Gondwana. Moreover, on the TDR and AS maps some basin contours were defined very efficiently, and as well as the main transform zones (Salado, Colorado, Ventana), minor transform zone (Rawson), and structural highs such as the Martín García, Tandil, del Plata, Rawson and Mar Argentino Rise were similarly effectively imaged.

Another key result of this study is the expression of the Palaeozoic Northern Magmatic arc of Patagonia based on the analytical signal and tilt angle. This late Palaeozoic arc is related to northward displacement of the Patagonia terrain prior to its collision with western Gondwana. This zone of weakness controlled the inception of the offshore Colorado basin during Mesozoic times and may have controlled the extension of the Colorado transform zone into the oceanic crust.

These results agree with previous studies based on seismic and gravimetric methods conducted in the Argentine continental passive volcanic margin region; for example, the delineation of the continental shelf edge by significant volcanic activity evidenced by the series of SDR wedges. These were identified in all the techniques employed and were especially marked in the 2-D Euler deconvolution solutions, which indicated SDR depths between 7000 and 9000 m according to Hinz *et al.* (1999).

The results, from the standard Euler 3-D deconvolution, provided information above the distribution of the deep faults in the Ventania-Cape fold-belt, that presented faults whose depth reached 6000-8000 m and dykes or sills around 14000 m deep; these probably are associated to the zones of accretion with Gondwana. Along the western edge of the Ameghino basin, both faults and dykes achieve depths from 2000 to 8000 m. These results are in good agreement with SVD as they display high-frequency patterns in the G anomaly and in the COT (depths from 2000 to 2500 m). In the Plata and Tandil basement highs the faults depths range from approximately 6000 to 10000 m. Moreover, the SDV and 3-D Euler deconvolution results were found to coincide because deeper sources (10000–14000 m) were calculated from the 3-D-Euler deconvolution in areas where the SDV exhibits high-frequency patterns, such as the G and Tona anomalies, the M series, the Martín García and Tandil basement highs and the Somuncurá massif. This can be

clearly seen in the northern magmatic arc and the inner alignments in some OBA. El Cortijo and Tandil sutures have some dykes and faults solutions deeper than 3000 m. These dykes are generally depicted in the results of all enhancement techniques.

In the Tona anomaly, the 2-D Euler deconvolution displayed few sources sub-parallel to the south edge of the Colorado basin for SI=0 and 1. However, sources sub-parallel to the continental edge displayed high frequencies, indicating deep sources, while the COT exhibited scattered high-frequency patterns.

The Tona anomaly is visible on the TDR map as the combined product of a deep source and a shallow one. One of them lies parallel to the margin and the other is parallel to the southern edge of the Colorado basin. The application of the Euler method to a 2-D profile revealed details about the depths of the sources responsible for the Tona anomaly up to the margin, which yielded better SDR depth results that are consistent with seismic-gravitational studies. The 2-D Euler method was used to calculate source depths of 8000–20000 m for the conspicuous Tona anomaly from a NW-trending profile.

In addition, a 2-D gravimetric inversion model based on a NE-trending profile was used to identify a mafic body along the Patagonia-Gondwana suture bounded by a sub-surface. This body may be an imbrication of the suture located in basement rocks.

Acknowledgements

To the following institutions, the Instituto de Geodesia y Geofísica Aplicadas (IGGA), School of Engineering of the Universidad de Buenos Aires, Instituto Geofísico Sismológico Volponi (IGSV) from the School of Physical and Natural Sciences of the Universidad Nacional de San Juan and the Instituto Universitario Naval (INUN), which have provided financial support for the Project PID Project B-ESCM - Caracterización geofisica y geodésica de la plataforma, borde continental y Cuenca Argentina a través del análisis de datos oceanográficos y métodos potenciales en el Océano Atlántico Sur (60ºW - 40ºW).

References

Amante, C., Eakins, B.W., 2009. ETOPO1 1 Arc-Minute Global Relief Model Procedures, Data Sources and Analysis. *NOAA Technical Memorandum NESDIS NGDC* -24, National Geophysical Data Center*, NOAA*, doi:10.7289/V5C8276M.

Arecco, M.A., Ruiz, F., Pizarro, G., Giménez, M. Martínez, M.P., Ramos, V.A., 2016 *a*. Gravimetric determination of the continental–oceanic boundary of the Argentine continental margin (from 36◦S to 50◦S), *Geophys. J. Int.,* 204, 366–385*.*

Arecco, M.A., Larocca, P.A., Oreiro, F., Pizarro, G., Ruiz, F., 2016 *b*. Estudio del margen continental argentino para la determinación del límite entre corteza oceánica y continental (desde 40ºS hasta 44ºS) a partir de métodos geomagnéticos. *Latinmag Letters*, Volume 6, Special Issue, Proceedings São Paulo, Brasil, A03, 1-7.

Austin, J.A., Uchupi, E., 1982. Continental–Oceanic crustal transition of southwest Africa. *AAPG Bull*. 66 (9): 1328–1347.

Baldi, J.E., Nevistic, V.A., 1996. Cuenca costa afuera del golfo San Jorge. Ramos, V. y Turic, M. (Eds.), XIII Congreso Geológico Argentino y III Congreso de Exploración de Hidrocarburos, Asociación Geológica Argentina e Instituto Argentino del Petróleo y el Gas, Relatorio (10): 171-192, Buenos Aires.

Blakely, R. 1996. Potential theory in gravity and magnetic applications. Cambridge University Press, London, 461pp.

Chernicoff, C.J., Zappettini, E.O., Peroni J., 2014. The Rhyacian El Cortijo suture zone: Aeromagnetic signature and insights for the geodynamic evolution of the southwestern Rio de la Plata craton, Argentina. *Geoscience Frontiers*, (5): 43–52.

Cingolani, C.A., 2011, The Tandilia System of Argentina as a southern extension of the Río de la Plata craton: An overview: *International Journal of Earth Sciences*, v. 100, p. 221–242. doi:10.1007/s00531-010-0611-5

Cingolani, C.A. and Dalla Salda, L., 2000. Buenos Aires cratonic region. In: Cordani, U., Milani, E., Thomaz Filho, A., Campos, D. (Eds.), Tectonic Evolution of South America. Proceedings 31st International Geological Congress, Río de Janeiro, pp. 139–146.

Cingolani, C.A., Santos, J.O.S., Griffin, W., 2010. New insights of the Palaeoproterozoic basement of Tandilia belt, Río de la Plata craton, Argentina: first Hf isotope studies on zircon crystals. In: Symposium GEOSUR, Extended Abstract, Mar del Plata, pp. 21–24.

Cooper, G.R.J. and Cowan, D.R., 2006. Enhancing potential field data using filters based on the local phase. *Comput. Geosci*., (32): 1585–1591.

Dalla Salda, L.H., Bossi, J. y Cingolani, C.A. 1988. The Rio de la Plata cratonic region of southwestern Gondwana. Episodes, 11, (4): 263-269.

Dalla Salda, L., 1987. Basement tectonics of the southern Pampean Ranges. *Tectonics* 6(3): 249-260.

Dalla Salda, L. and Francese, J., 1985. Los granitoides de Tandil. In: 1° Jornadas Geológicas Bonaerenses, Comisión Investigaciones Científicas de la provincia de Buenos Aires: 845-861, La Plata.

Dalla Salda, L.H., Bossi, J. y Cingolani, C.A. 1988. The Rio de la Plata cratonic region of southwestern Gondwana. Episodes, 11 (4): 263-269.

Durrehim, R.J. and Cooper, G.R.J., 1998. EULDEP: a program for the Euler deconvolution of magnetic and gravity data. *Computers & Geosciences* 24, (6): 545-550.

Ewing, M., Ludwig, W.J., Ewing, J.I., 1963. Geophysical investigations in the submerged Argentine coastal plain. Part 1. Buenos Aires to Peninsula Valdez. *Geological Society of America Bulletin*, (74): 275–292.

Fragoso-Cesar, A.R.S., 1980. O Cráton do Rio de la Plata e o Cinturão Dom Feliciano no Escudo Uruguaio-Sul-Riograndense. In: Congresso Brasileiro de Geologia, 31 SBG, vol. 5. Anais, Camboriú, 2879-2892.

Franke, D., Neben, S., Ladage, S., Schreckenberger, B., Hinz, K., 2007. Margin segmentation and volcano-tectonic architecture along the volcanic margin off Argentina/Uruguay, South Atlantic. *Marine Geology*, Vol. 244 (1-4): 46–67.

Fryklund, B., Marshall, A., Stevens, J., 1996. Cuenca del Colorado. In: Ramos, V. y Turic, M. (Eds.), XIII Congreso Geológico Argentino y III Congreso de Exploración de Hidrocarburos, Asociación Geológica Argentina e Instituto Argentino del Petróleo y el Gas, Relatorio (8): 135–158.

Ghidella, M.E., Chernicoff, C.J., Köhn, J., Kostadinoff, J., Gianibelli, J. C., 2005. Anomalías magnéticas en la provincia de Buenos Aires: compilación digital y principales unidades estructurales. In 15º Congreso Geológico Argentino, Cabaleri N., Cingolani, C.A, Linares, E., López de Luchi, M.G., Ostera, H.A. and Panarello, H.O. (eds.). In CD-ROM, Nº 161, 8 pp.

Gunn, P., 1975. Linear transformations of gravity and magnetic fields. *Geophysical Prospecting*, 23 (2): 300–312.

Hinz, K., Neben, S., Schreckenberger, B., Roeser, H.A., Block, M., Goncalves De Souza, K., and Meyer, H., 1999. The Argentine continental margin north of 48ºS: sedimentary successions, volcanic activity during breakup, *Marine and Petroleum Geology*, (16): 1–25.

Introcaso, A. 1980. A gravimetric interpretation of the Salado Basin (Argentina), *Bollettino di Geofisica Teorica ed Applicata*, 22, (87): 187-200.

Introcaso, A. 2003. Significativa descompensación isostática en la Cuenca del Colorado (República Argentina). *Revista de la Asociación Geológica Argentina*, 58 (3): 474-478.

Introcaso, A., Ghidella, M.E., Ruiz, F., Crovetto, C.B., Introcaso, B., Paterlini, C.M., 2008. Métodos gravi-magnetométricos modernos para analizar las características estructurales de la plataforma continental argentina. *Geoacta*, (33): 1-20.

Introcaso, A and Ramos, V.A, 1984. La cuenca del Salado. Un modelo de evolución aulacogénica. In: 9° Congreso Geológico Argentino. Actas (3): 27-46.

Kay, S.M., Ramos, V.A. Mpodozis, C., Sruoga, P., 1989. Late Paleozoic Jurassics silicic magmatism at the Gondwana margin: Analogy to the Middle Proterozoic in North America? *Geology*, (17): 324-328.

Lefort, J.P., Max, M.D., Roussel, J., 1988. The north-west boundary of Gondwanaland and its relationship with two satellite sutures Geophysical evidence. Evolution of the Caledonide-Appalachian Orogen. *Geol. Soc. Lond. Spec. Pub.,* (38): 49-60.

López de Lucchi, M.G., Rapalini, A.E., Tomezzoli, R.N., 2010. Magnetic fabric and microstructures of Late Paleozoic granitoids from the North Patagonian Massif: evidence of a collision between Patagonia and Gondwana? *Tectonophysics.* 494 (1-2): 118-137.

Malumián, N. and Ramos, V., 1984. Magmatic intervals, transgression-regression cycles and oceanic events in the Cretaceous and Terceary of southern South *America, Earth Planet. Sc. Let.* (67): 228-237.

Marinelli, R.V., Franzin, H.J., 1996. Cuencas de Rawson y península Valdés. In: Ramos, V. y Turic, M. (Eds.), XIII Congreso Geológico Argentino y III Congreso de Exploración de Hidrocarburos, Asociación Geológica Argentina e Instituto Argentino del Petróleo y el Gas, Relatorio (9):159-169.

Max, M.D., Ghidella, M.E., Kovacs, L., Paterlini, M., Valladares, J.A., 1999. Geology of the mainland Argentine continental shelf and margin from aeromagnetic survey. *Marine Petroleum Geology*, (16): 41-64.

Meyer, B., Saltus R., Chulliat A., 2016. EMAG2: Earth Magnetic Anomaly Grid (2-arc-minute resolution) Version 3. *National Centers for Environmental Information*, NOAA. Model. doi:10.7289/V5H70CVX.

Miller, H.G. and Singh, V., 1994. Potential field tilt-A new concept for location of potential field sources. *J. Appl. Geophys,* (32): 213–217.

Milligan, P.R. and Gunn, P.J., 1997. Enhancement and presentation of airborne geophysical data 1. *Journal of Australian Geology & Geophysics*, 17, (2): 63-75.

Mushayandebvu, M. F., van Driel, P., Reid, A.B., and Fairhead, J.D., 2001, Magnetic source parameters of two-dimensional structures using extended Euler deconvolution: Geophysics, (66): 814-823.

Nabighian, M.N., 1972. The analytic signal of two-dimensional magnetic bodies with polygonal cross section: its properties and use for automated interpretation. *Geophysics*, (37): 507–517.

Nabighian, M.N., 1984. Toward a three-dimensional automatic interpretation of potential field data via generalized Hilbert transforms: fundamental relations, *Geophysics*, (49): 780–786.

Nabighian, M.N, Grauch, V.J.S., Li, Y., Peirce, J.W., Phillips, J.D., Ruder, M.E., 2005. The historical development of the magnetic method in exploration. *Geohphysics*, (70), 6: P33ND-61ND.

Pankhurst, R.J., Ramos, A., Linares, E., 2003. Antiquity of the Río de la Plata Craton in Tandilia, southern Buenos Aires province, Argentina. *Journal of South American Earth Sciences,* 16 (1): 5-13.

Pángaro, F., Ramos, V.A., Kohler, G., 2011. Las cuencas del Colorado y Salado: nueva interpretación sobre su origen y su impacto en la configuración del Gondwana durante el paleozoico. In: XVIII Congreso Geológico Argentino, Neuquén. Abstracts on CD, 117-118.

Pángaro, F. and Ramos, V.A., 2012. Paleozoic crustal blocks of onshore and offshore central Argentina: New pieces of the southwestern Gondwana collage and their role in the accretion of Patagonia and the evolution of Mesozoic south Atlantic sedimentary basins. *Marine and Petroleum Geology*, (37): 162-183.

Paton, D.A., Mortimer, E.J. Hodgson, N., Van Der Spuy, D., 2016. The missing piece of the South Atlantic jigsaw: when continental break-up ignores crustal heterogeneity, Lyell Collection, The Geological Society of London. Special Publications.

Pizarro, G, Arecco, M.A. Ruiz, F., Ghidella, M. 2016. Modelado 3D por inversión gravimétrica de cuencas off shore de Argentina. *Geoacta*, 40, (2): 11-27.

Rabinowitz, P.D., LaBrecque, J., 1979. The Mesozoic South Atlantic Ocean and evolution of its continental margins. *J. Geophys. Res*., (84): 5973-6002.

Ramos, V.A., 1988. Late Proterozoic-Early Paleozoic of South America - a Collisional History. Episodes, 11, (3): (168-174).

Ramos, V.A., Riccardi, A.C. y Rolleri, E.O., 2004. Límites naturales del norte de la Patagonia. Revista de la Asociación Geológica Argentina, 59 (4): 785-786.

Ramos, V.A., 1996. Evolución tectónica de la Plataforma Continental, Geología y Recursos de la Plataforma Continental, In: Ramos, V. y Turic, M. (Eds.), Relatorio del XIII Congreso Geológico Argentino y III Congreso de Exploración de Hidrocarburos, Asociación Geológica Argentina e Instituto Argentino del Petróleo y el Gas, Relatorio (21): 385-404.

Ramos, V.A., 2008. Patagonia: A paleozoic continent adrift? *Journal of South American Earth Sciences,* (26): 235–251.

Ramos, V.A., Chemale, F., Naipauer, M., Pazos, P.J., 2014. A provenance study of the

Paleozoic Ventania System (Argentina): Transient complex sources from Western and Eastern Gondwana, *Gondwana Research*, (26): 719–740.

Rapallini, A., 2005. The accretionary history of Southern South America from the latest Proterozoic to the Late Palaeozoic: some palaeomagnetic Constraints, Terrane Processes at the Margins of Gondwana, *Geological Society of London, Special Publication*, (246): 305-328.

Rapella, C., Pankhurst, R., 1993. El volcanismo riolítico del noreste de la Patagonia: Un evento meso-jurásico de corta duración y origen profundo. In: XII Congreso Geológico Argentino y II Congreso de Exploración de Hidrocarburos, Actas (4): 179-188, Mendoza.

Reid, A.B., Allsop, J., Granser, H., Millett, A., Somerton, I., 1990. Magnetic interpretation in three dimensions using Euler Deconvolution. *Geophysics* 55, (1): 80-91.

Reid, A.B., Fitz Gerald, D., McInerney, P., 2003. Euler deconvolution of gravity data. In: Society of Exploration Geophysicists (SEG), Annual Meeting, 580-583, New Orleans, 13-18 September.

Riley, T. R., Flowerdew, M. J., Pankhurst, R. J., Curtis, M. L., Millar, I. L., Fanning, C. M. and Whitehouse, M. J. 2016. Early Jurassic magmatism on the Antarctic Peninsula and potential correlation with the Subcordilleran plutonic belt of Patagonia. *Journal of the Geological Society,* (174): 365-376, doi:10.1144/jgs 2016-053.

Rolleri, E.O., 1972. Acerca de la dorsal del Mar Argentino y su posible significado geológico. IN: V Congreso Geol. Arg., Actas (4): 203-220.

Ruiz, F. and Introcaso, A., 2011. Study of the Claromecó basin from gravity, magnetic and geoid ondulation charts. *Boletín del Instituto de Fisiografía y Geología*, 79-81.

Salem, A. and Smith, R., 2005. Depth and structural index from normalized local wavenumber of 2-D magnetic anomalies. *Geophysical Prospecting*, (53): 83–89.

Sylwan, C., 2001. Geology of the Golfo San Jorge Basin, Argentina. *Journal of Iberian Geology*, (27): 123-157.

Talwani, M., J. L. Worzel, and M. Landisman, 1959. Rapid gravity computations for two-dimensional bodies with application to the Mendocino submarine fracture zone. J. Geophys. Res., 64: 49-59.

Tankard, A. J., Uliana, M. A., Welsink, H. J., Ramos, V. A., Turic, M., França, A. B., Milani, E. J., de Brito Neves, B. B., Eyles, N., Skarmeta, J., Santa Ana, Wiens, F., Cirbian, M., Lopez, O. P., De Wit, G. J. B., Machacha, T. and McG. Miller, R., 1995. Structural and Tectonic Controls of Basin Evolution in Southwestern Gondwana during the Phanerozoic. AAPG Special Volumes. In: Tankard A. J., Suárez Soruco, R. & Welsink, H. J., (Eds.), Petroleum basins of South America. Am. Assoc. Pet. Geol. Mem., (62): 5-52.

Tavella, G.F. and Wrigth, C., 1996. Cuenca del Salado, Geología y Recursos de la Plataforma Continental. In: Ramos, V. y Turic, M. (Eds.), Relatorio del XIII Congreso Geológico Argentino y III Congreso de Exploración de Hidrocarburos, Asociación Geológica Argentina e Instituto Argentino del Petróleo y el Gas, Relatorio (6): 95-116.

Teruggi, M.E., Leguizamón, M.A., and Ramos, V.A., 1988, Metamorfitas de bajo grado con afinidades oceánicas en el basamento de Tandil: Su implicancia geotectónica, Provincia de Buenos Aires, *Revista Asociación Geológica Argentina*, 43, (3): 366–374.

Thompson, D.T., 1982. EDULDPH: A new technique for making computer-assisted depth estimates from magnetic data. *Geophysics*, 47, (1): 31–37.

Urien, C.M. and Zambrano, J.J., 1974. The Geology of the Basins of the Argentine Continental Margin and Malvinas Plateau, The South Atlantic, ed. Springer, 135-169.

Varela, R., Cingolani, C., Dalla Salda, L., 1988. Geocronología Rb/Sr en granitoides del basamento de Tandil, provincia de Buenos Aires. In: 2ª Jornadas Geológicas bonaerenses. Resúmenes: 291-304, Bahía Blanca.

Verduzco, B., Fairhead, J.D., Green, C.M., MacKenzie, C., 2004. New insights to magnetic derivatives for structural mapping. *Leading Edge*, (23): 116–119.

Zambrano J.J., 1974, Cuencas sedimentarias en el subsuelo de la provincia de Buenos Aires y zonas adyacentes. *Revista de la Asociación Geológica Argentina*, 29, (4): 443-469.